Journal of Sound and Vibration (2000) **234**(4), 577–589
doi:10.1006/jsvi.1999.2796, available online at http://www.idealibrary.com on IDEAL®

EFFECT OF HIGH-FREQUENCY EXCITATION ON NATURAL FREQUENCIES OF SPINNING DISCS

M. H. Hansen

Department of Solid Mechanics, Technical University of Denmark, DK-2800 Lyngby, Denmark

(*Received* 4 *May* 1999, *and in final form* 18 *November* 1999)

The effect of high-frequency, non-resonant parametric excitation on the low-frequency response of spinning discs is considered. The parametric excitation is obtained through a non-constant rotation speed, where the frequency of the pulsating overlay is much higher than the lowest natural frequencies. It is shown analytically and numerically that this excitation has the non-trivial effect of increasing these natural frequencies with increasing pulsation amplitude.

1. INTRODUCTION

Non-trivial effects of high-frequency parametric excitation on the low-frequency dynamics of spinning annular discs are considered. The disc is either clamped at the inner radius and free at the rim (a *clamped-free* disc) or *vice versa* (a *free-clamped* disc). It is shown that natural frequencies of the lower modes of a disc can be increased through high-frequency parametric excitation.

Current designs of circular saws and computer disk drives tend towards the use of thinner and higher speed discs. Decreased disc thickness reduces the bending stiffness and thereby the critical rotation speed of spinning discs. High speeds mean operating close to this critical rotation speed. Spinning discs subjected to a stationary transverse force, for example from the cutting process or the record-write head, lose the stability of the plane equilibrium at its critical rotation speed (e.g., references [1, 2]). This so-called *critical speed resonance* has recently been studied in detail by Raman [3]. Furthermore, higher speeds increase the aerodynamic pressure on spinning discs which also may cause instabilities (e.g., references [4–6]). Alternative methods to increase the critical rotation speed of spinning discs, without compromising the thickness requirements, are therefore interesting.

High-frequency excitation, or *fast excitation*, can have non-trivial effects on the linear and non-linear properties of mechanical systems. In particular, the linear stiffness about an equilibrium position may be increased through fast parametric excitation. The classical example is the stabilization of the inverted position of the planar pendulum (the *Kapitza Pendulum* [7]). Many other studies considering stability of systems subjected to fast excitation have been conducted; see, for example Blekhman [8] and the recent works by Jensen [9–11]. Experimental reproduction of these effects for an axially loaded beam has also recently been given by Jensen *et al.* [12].

A general mathematical tool for dealing with fast excited systems called the method of direct partition of motion (DPM) was provided by Blekhman [8]. To understand and model the effect of the fast excitation, he suggested the separation of the fast component of the motion, driven by the excitation, from the slow component of the motion. Using the method of DPM, one can obtain an equation governing this slow motion only, the *equation*

0022-460X/00/290577 + 13 $35.00/0

of slow motion. Herein, the average effect of the fast excitation is reduced to a fictive force, which Blekhman called the *vibrational force*.

Tcherniak and Thomsen [13] suggested an alternative approach to obtain the equation of slow motion based on a modified method of multiple scales. The concept is similar to DPM: separate the fast and the slow motions to obtain the average effect of the fast excitation. Tcherniak [14] used this alternative approach to show the influence of fast excitation on a continuous system: a simply supported beam with distributed fast excitation force. He separated the fast and slow components of the governing field equation for the beam without first performing a discretization. He thereby obtained an equation of slow motion in which the vibrational force was given in a continuous form. This continuous form allowed direct analysis of the effect of changes in the distribution of the fast force, and provide greater physical understanding of the problem.

This paper deals with another example of non-trivial effects of fast excitation on a continuous system: a spinning annular disc clamped at one rim and free at the other. The fast parametric excitation is obtained by a non-constant rotation speed. This system has been considered by Young [15], although he studied resonance phenomena whereas this study deals only with non-resonant motion. In a similar approach to that of Tcherniak [14], the equation of slow motion for the system and vibrational force are obtained in a continuous form using the modified methods of multiple scales. An analysis of slow motion is conducted which shows that the vibrational force adds positive-definite linear stiffness to the disc about its plane equilibrium. The equation of slow motion is then discretized using Galerkin's procedure. The lower natural frequencies of the spinning disc are thereby determined which show the stiffening effect of the pulsating rotation speed. Numerical simulations based on a finite difference approximation are performed and confirm the analytical results from the separation of motion.

2. THE MODEL

Consider the disc configuration in Figure 1. An annular disc of thickness h, inner radius r_i and outer radius r_o is considered. The disc is thin ($h \ll r_o$) and isotropic with Young's modulus E, the Poisson ratio v and density ρ. The disc is either clamped at the inner radius and free at the outer rim, or *vice versa*. It is rotating with the non-constant speed

$$\Omega_d = \Omega_0(1 + a \sin \Omega_v t), \tag{1}$$

where the amplitude of the speed variation is small $a \ll 1$, and the frequency is large compared to the lower natural frequencies of the disc. The critical rotation speed of spinning discs is of the same order as the lower natural frequencies (e.g., references [1, 16]); thus, at subcritical mean speeds: $\Omega_v \gg \Omega_0$.

The position of a material point P on the midplane of the disc is described in a *co-rotating disc fixed frame* as (R, θ, W), where W is the transverse displacement of the point. Note that it is thereby assumed that the deflection of the midplane is parallel to the Z-axis.

The linear field equation governing small transverse vibrations ($W \ll h$) of a thin spinning disc is given by the linearized classical plate theory and can be found in several papers on the subject (e.g., references [4, 17]). The governing field equation can be written in a non-dimensional form as

$$w_{,\tau\tau} + \eta \nabla^4 w_{,\tau} + \alpha \nabla^4 w + K[w] = 0, \tag{2}$$

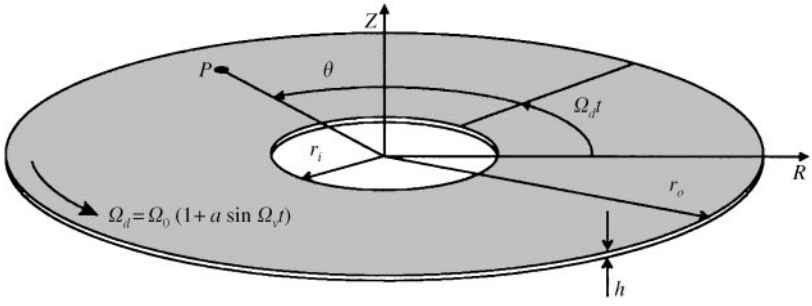

Figure 1. Disk spinning at a non-constant speed and the disk fixed co-ordinate system.

where the linear operator K describing the transverse component of membrane stresses can be written as

$$K[w] = -\frac{1}{r}(r\sigma_{rr}w_{,r})_{,r} - \frac{1}{r^2}(\sigma_{\theta\theta}w_{,\theta})_{,\theta} - \frac{1}{r}(\sigma_{r\theta}w_{,\theta})_{,r} - \frac{1}{r}(\sigma_{r\theta}w_{,r})_{,\theta}, \tag{3}$$

and the non-dimensional variables are given as

$$w = \frac{W}{h}, \qquad r = \frac{R}{r_o}, \qquad \tau = t\Omega_0, \qquad \sigma = \frac{\sigma^*}{\rho\Omega_0^2 r_o^2},$$

$$\kappa = \frac{r_i}{r_o}, \qquad \alpha = \frac{Eh^2}{12(1-\nu^2)\rho\Omega_0^2 r_o^4}, \qquad \eta = \eta^*\Omega_0\alpha, \qquad \Omega = \frac{\Omega_v}{\Omega_0}, \tag{4}$$

where σ^* is dimensional stress, κ is the radius ratio of the annular disc, α is the ratio between the bending stiffness and the mean restoring force due to the centrifugal stresses, and the non-dimensional excitation frequency is large, $\Omega \gg 1$.

The boundary conditions for the transverse deflection at the clamped rim are

$$w = 0 \quad \text{and} \quad w_{,r} = 0 \tag{5a}$$

and at the free rim

$$w_{,rr} + \nu\left(\frac{1}{r^2}w_{,\theta\theta} + \frac{1}{r}w_{,r}\right) = 0 \quad \text{and} \quad (\nabla^2 w)_{,r} + \frac{1-\nu}{r^2}\left(w_{,r} - \frac{w}{r}\right)_{,\theta\theta} = 0 \tag{5b}$$

which model the vanishing moment and effective shear force. Additionally, circumferential periodicity $w(r, \theta, \tau) = w(r, \theta + 2\pi, \tau)$ must be satisfied.

The non-dimensional membrane stresses due to the centrifugal and angular acceleration of the disc elements, are derived in Appendix A. The stresses satisfy the inplane equilibrium equations, neglecting inplane accelerations, and the boundary conditions of vanishing displacement on the clamped edge and vanishing radial normal and shear stress on the free edge. The stresses are axisymmetrical and can be written as

$$\sigma_{rr} = f_{rr}(r)(1 + a\sin\Omega\tau)^2, \qquad \sigma_{\theta\theta} = f_{\theta\theta}(r)(1 + a\sin\Omega\tau)^2, \qquad \sigma_{r\theta} = f_{r\theta}(r)\, a\Omega\cos\Omega\tau, \tag{6}$$

where f_{ii} are radial functions given in Appendix A.

The higher modes of the disc may be excited by the high-frequency parametric excitation given by operator (3) and stresses (6). In the following separation of motion it is presumed that such resonances with the higher modes do not occur. Frequency-dependent structural damping is assumed to suppress these resonances in the real disc. This type of structural damping can be modelled by *internal* viscoelastic damping, $\eta\nabla^4 w_{,\tau}$, which is proportional to the rate of change in the bending strains. Structural dissipation due to frictional losses at the clamping interface is also assumed to be modelled by the viscoelastic damping.

3. SEPARATION OF FAST AND SLOW MOTION

The governing field equation (2) with stresses (6) can be written as

$$w_{,\tau\tau} + \eta\nabla^4 w_{,\tau} + \alpha\nabla^4 w + L_c[w] = -L_c[w]\,(2a\sin\Omega\tau + a^2\sin^2\Omega\tau) + L_a[w]\,a\Omega\cos\Omega\tau, \tag{7}$$

where

$$L_c[w] = -\frac{1}{r}(rf_{rr}w_{,r})_{,r} - \frac{1}{r^2}f_{\theta\theta}w_{,\theta\theta} \quad \text{and} \quad L_a[w] = \left(\frac{1}{r}(f_{r\theta}w)_{,r} + \frac{1}{r}f_{r\theta}w_{,r}\right)_{,\theta}, \tag{8}$$

where L_c and L_a are linear stiffness operators modelling the transverse components of stresses due to the centrifugal acceleration and the angular acceleration respectively.

Equation (7) is a non-autonomous partial differential equation. The time-dependent terms on the right-hand side (r.h.s.) are called the *fast forces* due to the high frequency ($\Omega \gg 1$). The left-hand side contains the inertial and *slow forces*, which in this case are viscoelastic damping, bending stiffness and stiffness due to the mean part of the centrifugal acceleration.

3.1. TIME SCALES AND SEPARATION OF MOTIONS

Following the procedure by Tcherniak and Thomsen [13], a small parameter $\varepsilon = \Omega^{-1} \ll 1$ is defined, and two time scales are introduced

$$T_0 = \Omega\tau = \varepsilon^{-1}\tau \quad \text{and} \quad T_1 = \tau, \tag{9}$$

where T_0 and T_1 are considered as independent, fast and slow, time scales. The time derivative thereby transforms to

$$\frac{\partial^i}{\partial\tau^i} = (\varepsilon^{-1}D_0 + D_1)^i, \quad \text{where} \quad D_j = \frac{\partial}{\partial T_j}, \quad j = 0, 1. \tag{10}$$

A perturbation solution to equation (7) in the form

$$w(r, \theta, T_0, T_1) = z(r, \theta, T_1) + \varepsilon\psi(r, \theta, T_0, T_1) + \varepsilon^2\psi_2(r, \theta, T_0, T_1) + \mathcal{O}(\varepsilon^3) \tag{11}$$

is sought. In this perturbation solution the dominating part $z(r, \theta, T_1)$ is the slow component of the motion, and the higher order ψ-terms are small overlays of *fast motion* on this *slow motion.*

3.2. MAGNITUDE ORDERING

The order of the slow forces is supposed to be $\mathcal{O}(1)$, except for the viscoelastic damping which is of order ε. The pulsation amplitude is small ($a = \mathcal{O}(\varepsilon)$), thus the last term on the r.h.s. of equation (7) is the dominating part of the fast forces. For the fast forces to affect the slow motion, this term must be of order ε^{-1} [13]. The product $aL_a[w]$ must therefore be of order 1.

To determine the order of $L_a[w]$, it is noted that the radial shape function of the shear stress field, $f_{r\theta}$, contains the term $1/r^2$ (see Appendix A, equation (26)). Assuming that $\kappa = \mathcal{O}(\varepsilon^{1/2})$ and noting that $\kappa \leqslant r \leqslant 1$, the shear stress is assumed to vary rapidly with r. This can be expressed as $f_{r\theta} = f_{r\theta}(r/\varepsilon)$, which when substituted into (8) shows that $L_a[w]$ is of order ε^{-1} and $aL_a[w] = \mathcal{O}(1)$.

This assumption, however, only holds for clamped–free discs. It is invalid for free–clamped discs, because the coefficient of $1/r^2$ in $f_{r\theta}$ in this case is equal to κ^4 (see Appendix A, equation (28)). Hence, the following separation of motion and analysis is only valid for a clamped–free disc.

3.3. EQUATION OF SLOW MOTION

Substitution of the perturbation solution (11) into the partial differential equation (7) and collection of terms of equal order yields the equation of order ε^{-1}:

$$D_0^2\psi = L_a[z]\, a\cos T_0 \tag{12}$$

with the solution

$$\psi(r, \theta, T_0, T_1) = -L_a[z]\, a\cos T_0 + T_0 c_1(r, \theta, T_1) + c_2(r, \theta, T_1), \tag{13}$$

where $c_1 = 0$ due to the boundedness of the solution as $T_0 \to \infty$. The solution $c_2(r, \theta, T_1)$ is contained in the slow motion $z(r, \theta, T_1)$ and can therefore be omitted. Equation (12) shows that the dominating part of the fast motion, ψ, is determined from an equilibrium between inertia forces and the excitation force. Damping and stiffness forces are neglected, thus the fast motion ψ is assumed to be *non-resonant* and in *anti-phase* with the excitation force.

Now that the fast motion is determined, its effect on the slow motion, z, can be determined from the equation of order ε^0:

$$D_0^2\psi_2 = -2D_0D_1\psi - D_1^2 z - \eta D_0 \nabla^4 z - \alpha\nabla^4 z - L_c[z] + L_a[\psi]\, a\cos T_0. \tag{14}$$

The second order part of the fast motion, ψ_2, is not needed. The condition that ψ_2 must be bounded for $T_0 \to \infty$ gives however an equation for determination of z. The right-hand side of equation (14) can be split into two parts: T_0-harmonic terms and terms with a non-vanishing T_0-average. The latter terms will create secular terms in the solution of equation (14). Hence, boundedness of ψ_2 requires that the T_0-average of the right-hand side is zero. Defining the T_0-average as $\langle\ \rangle = (2\pi)^{-1}\int_0^{2\pi}(\,)\,\mathrm{d}T_0$, this condition reduces to

$$D_1^2 z + \eta\boldsymbol{\nabla}^4 D_1 z + \alpha\boldsymbol{\nabla}^4 z + L_c[z] = \langle L_a[\psi]\, a\cos T_0\rangle. \tag{15}$$

Substituting the solution for ψ into this equation yields the equation of slow motion

$$z_{,rr} + \eta\boldsymbol{\nabla}^4 z_{,r} + \alpha\boldsymbol{\nabla}^4 z + L_c[z] = -\tfrac{1}{2}a^2 L_a^2[z], \tag{16}$$

where the right-hand side describes the slow force due to the fast excitation of the disc. This force is the *vibrational force* [8].

The non-autonomous equation (7) governing the full motion of the disk is reduced to an autonomous partial differential equation (16) governing only the dominating slow part of the disc motion. In this equation the average effect of the fast forces is given by the vibrational force. Similar to the analysis of the effect of high-frequency pulsating fluid flow in a cantilever pipe by Jensen [9], the magnitude of this force is independent of the excitation frequency and depends only on the pulsation amplitude.

4. ANALYSIS OF SLOW MOTION

For both critical speed resonance and aeroelastic instabilities, the dominating part of the response is low-frequency slow motion (e.g., references [1, 5]). This slow motion is the motion of interest, and the fast motion due to the fast excitation is only of second order interest, as formulated by the perturbation solution (11). Through the separation of fast and slow motion, the effect of the fast excitation on the low-frequency response can now be analyzed using the autonomous equation of slow motion (16).

4.1. POSITIVE DEFINITENESS OF THE VIBRATIONAL FORCE

It is first shown that the fast parametric excitation always adds stiffness to the disc. This is done by proving that the operator of the vibrational force $a^2L_a^2$ is positive definite.

Let the domain of the disc be $\mathscr{D} = \{(r, \varphi)\colon \kappa \leqslant r \leqslant 1, 0 \leqslant \varphi < 2\pi\}$, and the space of complex-valued functions on $\mathscr{D}$ be denoted as $(\mathbb{C}, \mathscr{D})$. An inner product on $(\mathbb{C}, \mathscr{D})$ is defined as

$$\langle u, v\rangle = \int_0^{2\pi}\int_\kappa^1 u\bar{v}r\,\mathrm{d}r\,\mathrm{d}\theta, \quad \forall u,\ v \in (\mathbb{C}, \mathscr{D}), \tag{17}$$

where the bar represents a complex conjugate. The subset of complex-valued functions with finite L_2-norm on $\mathscr{D}$ which satisfy boundary conditions (5) is denoted as $L_2^*(C, \mathscr{D})$. It can be shown by partial integration and use of boundary conditions that the spatial operators $\mathbf{V}^4$ and K of the governing equation (2) are both self-adjoint. The operator L_a is therefore also self-adjoint and symmetric. Thus the operator of the vibrational force L_a^2 is positive definite, because the symmetry of L_a gives

$$\langle u, a^2L_a^2[u]\rangle = a^2\langle L_a[u], L_a[u]\rangle > 0, \quad \forall u \in L_2^*(\mathbb{C}, \mathscr{D}) \tag{18}$$

which shows that the stiffness due to the vibrational force is positive definite.

4.2. GALERKIN DISCRETIZATION

The circumferential periodicity condition means that any transverse deflection of the disc can be described exactly by the Fourier series:

$$z(r, \theta, \tau) = \sum_{n=0}^{\infty} (\Psi_n^c(r, \tau)\cos n\theta + \Psi_n^s(r, \tau)\sin n\theta), \tag{19}$$

where Ψ_n^c and Ψ_n^s are coefficient functions of the series and depend on radius r and time τ. Note that the subscript n denotes the number of nodal diameters of the modes.

The substitution of equation (19) into equation (16) and collection of terms of equal harmonics gives two identical and uncoupled equations for the sine and cosine mode coefficient functions, Ψ_n^s and Ψ_n^c. Because the coefficient functions are uncoupled, the superscripts are omitted, and the equation for each n can be written as

$$\ddot{\Psi}_n + \eta K_{b;n}^r[\dot{\Psi}_n] + \alpha K_{b;n}^r[\Psi_n] + L_{c;n}^r[\Psi_n] - \tfrac{1}{2}n^2a^2L_a^{r^2}[\Psi_n] = 0, \tag{20}$$

where the radial operators (with superscript r) become

$$K_{b;n}^r[\Psi_n] = \left(\frac{\partial^2}{\partial r^2} + \frac{1}{r}\frac{\partial}{\partial r} - \frac{n^2}{r^2}\right)^2 \Psi_n, \qquad L_{c;n}^r[\Psi_n] = -\frac{1}{r}(rf_{rr}\Psi_{n,r})_{,r} + \frac{n^2}{r^2}f_{\theta\theta}\Psi_n,$$

$$L_a^r[\Psi_n] = \frac{1}{r}(f_{\theta\theta}\Psi_n)_{,r} + \frac{1}{r}f_{r\theta}\Psi_{n,r}. \tag{21}$$

To obtain the corresponding radial boundary conditions for Ψ_n, expansion (19) must be inserted into equation (5).

The coefficient function $\Psi_n(r, \tau)$ is approximated by the finite expansion of the radial eigenfunctions $R_{mn}(r)$ of the stationary disk [18]:

$$\Psi_n(r, \tau) \approx \sum_{m=0}^{M} q_{mn}(\tau)\, R_{mn}(r), \tag{22}$$

where m denotes the number of nodal circles of the mode (m, n). Substitution of equation (22) into equation (20), multiplication with $R_{ln}(r)$, integration over r as $\int_\kappa^1(\,)r\,\mathrm{d}r$, and insertion of a solution in the form $q_{mn}(r, \tau) = d_{mn}\,\mathrm{e}^{\lambda\tau}$ yield algebraic eigenvalue problems for each n:

$$(\mathbf{M}_n\lambda^2 + \mathbf{C}_n\lambda + \mathbf{S}_n)\,\mathbf{d}_n = \mathbf{0}, \tag{23}$$

where $\mathbf{M}_n = \mathbf{I}, \mathbf{C}_n, \mathbf{S}_n$ are mass, damping and stiffness matrix, respectively, and $\mathbf{d}_n = \{d_{0n}, d_{1n}, \ldots\}^{\mathrm{T}}$ is a displacement vector. The damping matrix $\mathbf{C}_n$ is diagonal with $c_{mm} = \eta k_{mn}^4$, where k_{mn} are the eigenvalues of the stationary disc. The elements of $\mathbf{S}_n$ are

$$s_{lm;n} = \alpha\delta_{lm}k_{mn}^4 + \int_\kappa^1 R_{ln}L_{c;n}^r[R_{mn}]\,r\,\mathrm{d}r + \frac{1}{2}a^2n^2\int_\kappa^1 L_a^r[R_{ln}]\,L_a^r[R_{mn}]\,r\,\mathrm{d}r, \tag{24}$$

where δ_{lm} is Kronecker's delta. The stiffness coefficient due to the vibrational force is clearly positive definite. Note that the vibrational force is zero for axisymmetrical modes $n = 0$.

4.3. NATURAL FREQUENCIES

The lower natural frequencies of the disc under the influence of the fast excitation are determined from the eigenvalue problem (23) as $\omega_{mn} = \mathrm{Im}\{\lambda_{mn}\}$. Figure 2 shows the undamped natural frequencies of the three lowest asymmetrical modes $m = 0$ and $n = 1, 2, 3$, as a function of pulsation amplitude a. The disc parameters are $\nu = 0{\cdot}3$, $\kappa = 0{\cdot}3$ and $\alpha = 0{\cdot}1$. A sufficient convergence of the frequencies (error $< 0{\cdot}1\%$) is obtained with two terms used in expansion (22). Note that no excitation frequency Ω has been given in this

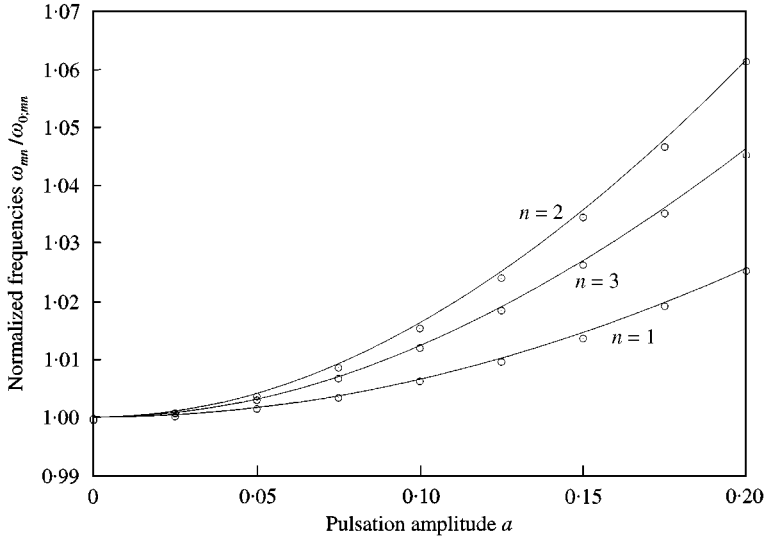

Figure 2. Normalized natural frequencies of lower asymmetrical modes of a clamped–free disk as a function of pulsation amplitude a for $\eta = 0$, $\nu = 0{\cdot}3$, $\kappa = 0{\cdot}3$ and $\alpha = 0{\cdot}1$. Points ○: Numerical simulations with $\Omega = 100$ and $\eta = 0.0003$ (section 5).

example because the vibrational force is only dependent on the pulsation amplitude. The points in Figure 2 are obtained from numerical simulations and presented in section 5.

The frequencies ω_{mn} are normalized with the frequencies of the unexcited disc $\omega_{0;mn}$. At a pulsation amplitude of 20% of the mean rotation speed ($a = 0{\cdot}2$), the maximum increase of the frequencies due to the fast excitation is 6%. This is for mode (0, 2) which has the largest slope. Frequency curves for modes with $n > 3$ have been computed and show that the slope decreases with mode number n.

The lower asymmetrical modes of the clamped–free discs are the critical modes in the case of *critical speed resonance* instabilities (e.g., references [1–3]) or aeroelastic instabilities (e.g., references [5, 6]). In both cases, the increased linear stiffness due to the fast parametric excitation can stabilize the plane equilibrium of a disc spinning faster than its critical speed. The rotation speed, in this case, cannot be far from the critical speed because the effect of fast excitation is small. However, the main aim of this analysis is not to solve the stability problem of spinning disc devices, but to show that fast excitation of spinning discs has unexpected effects on the linear stiffness of its lower modes.

5. NUMERICAL ANALYSIS OF THE FULL MOTION

To check the analytical results of the separation of motion, these are compared to a numerical solution of the full equation of motion (7).

5.1. NUMERICAL MODEL

The numerical solution is based on a finite difference approximation of the governing equations for the coefficients functions of the sine and cosine modes. Substitution of the circumferential expansion (19) into equation (7) and collecting terms of equal harmonics

gives

$$\ddot{\Psi}^s_n + \eta K^r_{b;n}[\dot{\Psi}^s_n] + \alpha K^r_{b;n}[\Psi^s_n] + L^r_{c;n}[\Psi^s_n](1 + a\sin\Omega\tau)^2 - nL^r_a[\Psi^c_n]\,a\Omega\cos\Omega\tau = 0,$$

$$\ddot{\Psi}^c_n + \eta K^r_{b;n}[\dot{\Psi}^c_n] + \alpha K^r_{b+n}[\Psi^c_n] + L^r_{c;n}[\Psi^c_n](1 + a\sin\Omega\tau)^2 + nL^r_a[\Psi^s_n]\,a\Omega\cos\Omega\tau = 0, \quad (25)$$

where the operators K^r_{b+n}, $L^r_{c;n}$ and L^r_a are given by equation (21). The boundary conditions for Ψ^s_n and Ψ^c_n are obtained by inserting equation (19) into equation (5). Unlike the equation of slow motion, the sine and cosine modes are now linearly coupled through the angular acceleration term. Because the coupling occurs between modes with equal mode number n, it is called an *intra-modal* coupling.

Two time-dependent vectors are defined to describe the coefficient functions, $\Psi^s_n(r, \tau)$ and $\Psi^c_n(r, \tau)$, in a finite number of points along a radial of the disc. Operators (21) and the boundary conditions are then approximated by simple central differences based on this discretization. These approximations are used to set up two sets of second order ordinary differential equations (ODEs) which are coupled through the intra-modal coupling. The full set of ODEs are then rewritten on a first order form so that they can be integrated with a Runge–Kutta–Verner fifth and sixth order method.

The separation of motion presumes non-resonant fast motion. This condition is assumed to be satisfied for a real disc where *primary* and *secondary* parametric resonances may be suppressed naturally by structural dissipation [19]. To model this structural dissipation, the regions of primary and secondary resonances in the (a, Ω)-plane are avoided by using a sufficient quantity of internal viscous damping, η, in the numerical simulations. *Combination* resonances that may occur in a parametrically excited multiple-degrees-of-freedom system cannot always be suppressed by viscous damping [19]. However, such resonances have not been encountered in the simulations.

5.2. COMPARISON OF ANALYTICAL AND NUMERICAL RESULTS

The curves in Figure 2 show the natural frequencies determined from the equation of slow motion (16). The points in Figure 2 represent frequencies obtained by numerical simulations. The comparison shows that the equation of slow motion describes the behaviour of these lower natural frequencies as a function of pulsation amplitude. A more detailed comparison of the analytically predicted and numerically integrated motion of the disc is now performed.

The two equations (25) with the intra-modal coupling lead to a natural separation of the fast and slow motions in the numerical simulations; the initial conditions of the numerical integration are chosen such that $\Psi^c_n(r, 0)$ is equal to the first eigenmode of equation (25) for $a = 0$, while $\Psi^s_n(r, 0) = \dot{\Psi}^s_n(r, 0) = \dot{\Psi}^c_n(r, 0) \equiv 0$. The dominant motion of the disc is thereby slow oscillations in the cosine mode, thus $z(r, \theta, \tau) = \Psi^c_n(r, \tau)\cos n\theta$. The sine mode will be excited by the fast excitation through the intra-modal coupling, i.e., the sine mode vibration describes the fast component of the disc motion, $\psi(r, \theta, \tau, \Omega\tau) = \Psi^s_n(r, \tau, \Omega\tau)\sin n\theta$. It is noted that the fast excitation due to the centrifugal acceleration is of order ε and has not shown any effect on the numerical results.

Figure 3 shows time history plots of the cosine mode (slow) and sine mode (fast) oscillations ($n = 2$) at the free outer rim $r = 1$ for a disc with $\nu = 0{\cdot}3$, $\kappa = 0{\cdot}3$ and $\alpha = 0{\cdot}1$. The internal damping is $\eta = 0{\cdot}001$, and the rotation speed has a pulsating overlay of $a = 0{\cdot}2$ and $\Omega = 100$.

The time histories of the cosine mode, with and without fast parametric excitation, are plotted. They clearly show the decrease in the period of oscillation due to the fast excitation.

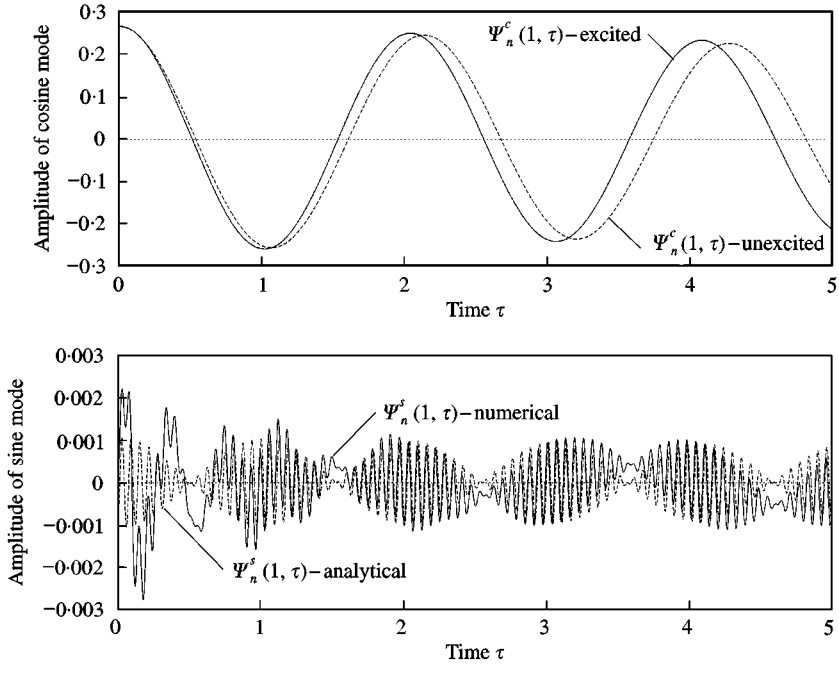

Figure 3. Time history plots of sine and cosine modes by numerical solution of equations (25) with $n = 2$, $a = 0{\cdot}2$, $\Omega = 100$ and $\eta = 0{\cdot}001$. The analytical time history of the sine mode vibration is obtained from equation (13).

The amplitude of the sine mode oscillations is approximately 100 times smaller than that of the slow motion, which agrees with the assumption that the fast motion is of order ε. The solid curve in the time history plots of the sine mode is obtained by the numerical integration, while the dashed curve represents the analytical solution for the fast motion (13). Except for some transient motion, the two curves almost coincide. Thus, the numerical integration of the full equation of motion supports the results of the separation of motion: the fast motion is in anti-phase with the fast excitation and has the amplitude and frequency given by equation (13).

The analytical separation of motion predicts that the effect of the vibrational force on the lower modes is independent of excitation frequency Ω. This is valid assuming that Ω is sufficiently large compared to the corresponding natural frequencies and that no resonant motion of higher modes occurs. Numerical simulations performed for different excitation frequencies, however, indicate that there is a dependency of the vibrational force on both Ω and the quantity of internal damping η.

The upper part of Figure 4 shows the point frequency response of the disc for modes with $n = 1$ and damping $\eta = 0$, $0{\cdot}0002$ and $0{\cdot}0004$. While the lower modes are almost unaffected by the internal damping, the highest modes in the frequency response are *over-damped*.

In the lower part of Figure 4, the normalized frequency of the cosine mode $(m, n) = (0, 1)$ is shown as a function of Ω for $a = 0{\cdot}1$ and two different damping coefficients $\eta = 0{\cdot}0002$ and $0{\cdot}0004$. After a few variations at low excitation frequencies, both sets of frequencies become independent of Ω and approach the analytical prediction shown by the dashed line. The amplitude of these variations are smaller for $\eta = 0{\cdot}0004$ than for $\eta = 0{\cdot}0002$. This indicates that the vibrational force becomes independent of the excitation frequency at a lower Ω for higher internal damping.

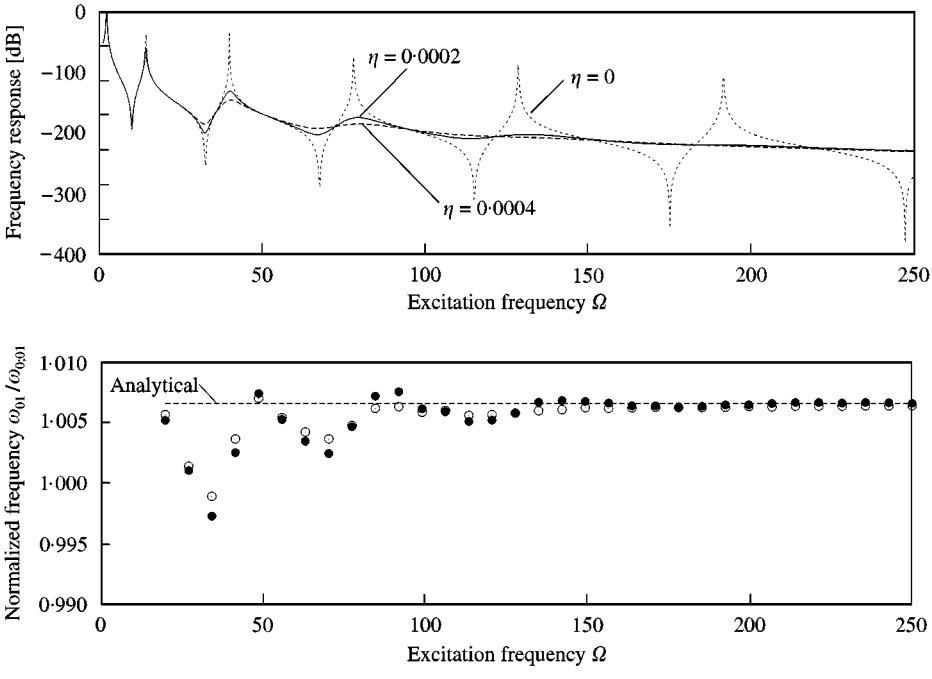

Figure 4. Top: Frequency response of the disk with $n = 1$, $\kappa = 0{\cdot}3$, $\nu = 0{\cdot}3$ and $\alpha = 0{\cdot}1$, computed for $\eta = 0$, 0·0002 and 0·0004. Bottom: Natural frequencies of mode (0,1) as a function of excitation frequency, Ω, obtained by numerical simulations for $\eta = 0{\cdot}0002$ (●) and $\eta = 0{\cdot}0004$ (○).

A comparison of the three frequency responses (upper part of Figure 4) to the frequency of the slow motion (lower part of Figure 4), shows that the vibrational force becomes independent of Ω in the range of over-damped modes. This observation agrees with the presumption made in the separation of motion that the fast motion is non-resonant. The variations of the frequency of slow motion may arise because this presumption fails in the lower frequency range for a particular amount of internal damping.

6. SUMMARY AND CONCLUSIONS

The effect of fast parametric excitation of spinning discs is considered analytically and numerically.

The parametric excitation is created by a non-constant rotation speed. The pulsating overlay of the rotation speed has a small amplitude but a very high frequency compared to the lower natural frequencies. A modified method of multiple scales is used to separate the motion of the disc into a fast and a slow component. Presuming that the "fast motion" is not in resonance with the fast excitation, an equation governing the "slow motion" is derived. Herein, the average effect of the fast excitation is presented by a "vibrational force" which is proportional to the square of the pulsation amplitude but independent of the excitation frequency.

The separation of motion is performed on operator form and it is shown that the vibrational force operator is positive definite. Natural frequencies of the lower asymmetrical modes are therefore increased as the pulsation amplitude is increased. Numerical

simulations based on a finite difference approximation of the equation of full motion confirm these natural frequencies obtained from the equation of slow motion. Furthermore, the numerical simulations show that the vibrational force is independent of excitation frequency as predicted by the separation of motion.

This work shows that there is a stiffening effect of fast parametric excitation of spinning discs. Although this increase in stiffness is shown to be small, this effect is unexpected and will not appear in a traditional analysis. Similar effects may arise for a spinning disc with fast kinematic excitation of its suspension, which is the topic of current research. Obviously, experiments are needed to confirm these non-trivial effects of fast parametric excitation of spinning discs.

ACKNOWLEDGMENTS

The author would like to thank I. I. Blekhman, J. J. Thomsen, D. Tcherniak and J. S. Jensen for many invaluable discussions and suggestions.

REFERENCES

1. Y. Honda, H. Matsusiha, and S. Sato 1985 *Journal of Sound and Vibration* **102**, 457–472. Modal response of a disk to a moving concentrated harmonic force.
2. I. Y. Shen and C. D. Mote, Jr. 1991 *Journal of Sound and Vibration* **148**, 307–318. On the mechanisme of instability of a circular plate under a rotating spring-mass-dashpot system.
3. A. Raman and C. D. Mote, Jr. 1999 *International Journal of Nonlinear Mechanics* **34**, 139–157. Non-linear oscillations of circular plates near a critical speed resonance.
4. H. Hosaka and S. H. Crandall 1992 *Acta Mechanica* **3**, 115–127. Self-excited vibrations of a flexible disk rotating on an air film above a flat surface.
5. C. D'Angelo and C. D. Mote Jr. 1993 *Journal of Sound and Vibration* **168**, 15–30. Aerodynamically excited vibration and flutter of a thin disk rotating at superpercritical speed.
6. M. H. Hansen, A. Raman and C. D. Mote, Jr. (in press) *Journal of Fluids and Structures*. Estimation of non-conservative aerodynamic pressure leading to flutter of spinning disks (submitted).
7. P. L. Kapitza 1951 *Zurnal Eksperimental'noj i Teoreticeskoj Fiziki* **21**, 588–597. Dynamic stability of a pendulum with an oscillating point of suspension (in Russian).
8. I. I. Blekhman 2000 *Vibrational Mechanics*. Moscow: Fizmatlit Publishing Company. World Scientific Publishing Company, Singapore.
9. J. S. Jensen 1999 *Nonlinear Dynamics*, **19**, 171–191. Articulated pipes conveying fluid pulsating with high frequency.
10. J. S. Jensen 1999 *International Journal of Nonlinear Mechanics* **35**, 217–227. Buckling of an elastic beam with added high-frequency excitation.
11. J. S. Jensen 1998 *Journal of Sound and Vibration* **215**, 125–142. Nonlinear dynamics of the follower-loaded double pendulum with added support excitation.
12. J. S. Jensen, D. Tcherniak and J. J. Thomsen (in press) *ASME Journal of Applied Mechanics* Non-trivial effects of fast harmonic excitation: experiments for an axially loaded beam.
13. D. Tcherniak and J. J. Thomsen 1998 *Nonlinear Dynamics* **17**, 227–246. Slow effects of fast harmonic excitation for elastic structures.
14. D. Tcherniak 1999 *Journal of Sound and Vibration* **227**, 343–360. The influence and utilization of fast excitation on a continuous system.
15. T. H. Young 1992 *American Society of Mechanical Engineers, Journal of Vibration and Acoustics* **114**, 506–513. Nonlinear transverse vibrations and stability of spinning disks with nonconstant spinning rate.
16. S. Chonan and S. Sato 1988 *Journal of Sound and Vibration* **127**, 245–252. Vibration and stability of rotating free–clamped slicing blades.
17. A. A. Renshaw, C. D'Angelo and C. D. Mote, Jr 1994 *Journal of Sound and Vibration* **177**, 577–590. Aerodynamically excited vibration of a rotating disk.

18. S. M. VOGEL and D. W. SKINNER 1965 *American Society of Mechanical Engineers, Journal of Applied Mechanics* **32**, 926–931. Natural frequencies of transversely vibrating uniform annular plates.
19. A. H. NAYFEH and D. T. MOOK 1979 *Nonlinear Oscillations*. New York: Wiley.
20. S. TIMOSHENKO and J. N. GOODIER 1951 *Theory of Elasticity*. New York: McGraw-Hill.

APPENDIX A: MEMBRANE STRESSES DUE TO A NON-CONSTANT ROTATION SPEED

The derivation of the resulting membrane stresses (6) is based on the assumption of *plane-stress*, negligible inplane material accelerations compared to the body forces, and compatible linearized Lagrangean strains, i.e., the effect of midplane stretching is neglected.

The procedure for the derivation is based on an Airy stress potential representation of the stresses. First, the radial and circumferential body forces due to the particular kinematic excitation are derived, yielding the inplane force equilibrium equations [20] in which the inplane material accelerations are neglected. Secondly, a stress function is defined such that these equilibria are satisfied. From the compatibility condition for the linear strains [20] and Hooke's law, a governing equation for the stress field is then given by the stress function. The boundary conditions of the stress field are vanishing radial and shear stress at the free rim, and vanishing radial and circumferential displacements at the clamping radius. Solving the linear governing equation for the stress field, and using superposition of the general solutions satisfying the compatibility condition [20], the membrane stresses (6) are obtained.

Non-dimensional body forces due to the centrifugal and angular acceleration through the non-constant rotation speed $(1 + a\sin\Omega\tau)$ of the disc, can be derived as

$$p_r = r\,(1 + a\sin\Omega\tau)^2, \qquad p_\theta = -\,r\,a\Omega\cos\Omega\tau.$$

These are axisymmetrical, and the derivations described above lead to the axisymmetrical stresses giving by equation (6). The radial dependencies of the stresses are

$$f_{rr}(r) = a_1 + \frac{a_2}{r^2} - \frac{1}{8}(3+\nu)r^2, \qquad f_{\theta\theta}(r) = a_1 - \frac{a_2}{r_2} - \frac{1}{8}(1+3\nu)\,r^2,$$

$$f_{r\theta}(r) = \frac{1}{4}\left(r^2 - a_3\frac{1}{r^2}\right), \tag{26}$$

where the constants a_1, a_2 and a_3 in the case of a clamped–free disc are

$$a_1 = \frac{1}{8}\frac{(1+\nu)((\nu-1)\kappa^4 - 3 - \nu)}{(\nu-1)\kappa^2 - 1 - \nu}, \qquad a_2 = \kappa^2\frac{1}{8}\frac{(1-\nu)((1+\nu)\kappa^2 - 3 - \nu)}{(\nu-1)\kappa^2 - 1 - \nu},$$

$$a_3 = 1 \tag{27}$$

and in the case of a free–clamped disc,

$$a_1 = \frac{1}{8}\frac{(4\nu + \nu^2 + 3)\kappa^4 - \nu^2 + 1}{(1+\nu)\kappa^2 + 1 - \nu}, \qquad a_2 = -\,\kappa^2\frac{1}{8}\frac{((-3 + 2\nu + \nu^2)\kappa^2 - \nu^2 + 1)}{(1+\nu)\kappa^2 + 1 - \nu},$$

$$a_3 = \kappa^4. \tag{28}$$